

## 浓缩生长因子联合骨髓间充质干细胞膜片的生物学性能 及其在骨缺损修复中的作用

石剑虹<sup>1,2</sup>, 田原野<sup>1</sup>, 陈楷<sup>1</sup>, 孙高<sup>1</sup>, 吴国民<sup>1</sup>

(1. 吉林大学口腔医院口腔颌面外科与口腔整形美容外科, 吉林 长春 130021; 2. 吉林大学口腔医院吉林省牙发育及颌骨重塑与再生重点实验室, 吉林 长春 130021)

**[摘要]** **目的:** 探讨浓缩生长因子(CGF)对骨髓间充质干细胞(BMSCs)膜片性能的影响, 并阐明含CGF复合细胞膜片(CS)在骨缺损修复中的作用。**方法:** 体外实验, 选取2只3周龄SD大鼠, 分离培养获得BMSCs, 茜素红和油红O染色鉴定BMSCs成骨和成脂能力。选取3只3周龄SD大鼠, 制备CGF液态提取物(CGF<sub>e</sub>), 将细胞分为对照组、传统CS(BMSC-CS)组和含CGF复合CS(CGF/BMSC-CS)组。HE染色观察2组CS形态表现, 茜素红和碱性磷酸酶(ALP)染色检测各组CS体外成骨情况, 细胞划痕实验检测各组细胞迁移能力, 实时荧光定量PCR(RT-qPCR)法检测各组细胞中ALP、胶原酶I型(COL-1)、Runt相关转录因子2(RUNX2)和骨钙蛋白(OCN)mRNA表达水平。体内实验, 选取15只SD大鼠随机分为对照组、BMSC-CS组和CGF/BMSC-CS组, 显微计算机断层扫描(Micro-CT)检测各组大鼠颅骨缺损处骨形成参数, HE染色和Masson染色观察各组大鼠颅骨缺损组织形态表现。**结果:** 第3代BMSCs为梭形, 排列紧密, 呈漩涡团簇状生长; 茜素红染色有明显的钙结节生成, 油红O染色有红色脂滴形成, 证实细胞具有良好的成骨和成脂分化的能力。CS为白色半透明状, 边缘轻微卷曲, 剥离后的CS卷曲皱缩为不规则状。与BMSC-CS组比较, CGF/BMSC-CS组CS白色更深, 透明程度较低, 在厚度和延展性方面明显增加, 不易破损, 有一定黏性和可塑性。HE染色观察, 与BMSC-CS组比较, CGF/BMSC-CS组CS细胞数增加, 排列密集, 细胞外基质(ECM)更丰富, 包裹连接细胞形成一个整体的片状结构。茜素红和ALP染色检测, 与对照组比较, BMSC-CS组CS的ALP活性和矿化提升值均明显升高( $P<0.05$ ); 与对照组和BMSC-CS组比较, CGF/BMSC-CS组CS成骨细胞及红色矿化结节数明显增多, 染色明显加深, 阳性面积增大, ALP活性和矿化提升值均明显升高( $P<0.05$ )。细胞划痕实验检测, 培养24 h, 与对照组比较, BMSC-CS组和CGF/BMSC-CS组细胞迁移率均明显升高( $P<0.05$ ); 与BMSC-CS组比较, CGF/BMSC-CS组细胞迁移率明显升高( $P<0.01$ ); 培养48 h, 与对照组比较, CGF/BMSC-CS组细胞迁移率明显升高( $P<0.05$ )。RT-qPCR法检测, 与对照组比较, BMSC-CS组细胞中COL-1和OCN mRNA表达水平均明显升高( $P<0.01$ ), CGF/BMSC-CS组细胞中ALP、COL-1、OCN和RUNX2 mRNA表达水平均明显升高( $P<0.01$ ); 与BMSC-CS组比较, CGF/BMSC-CS组细胞中ALP、COL-1和OCN mRNA表达水平均明显升高( $P<0.01$ )。Micro-CT检测, 对照组大鼠颅骨缺损区域边界清晰, 几乎无新骨生成; BMSC-CS组大鼠颅骨仅在骨缺损边缘有少量新骨形成, 缺损中心区域有明显空缺; CGF/BMSC-CS组大鼠颅骨新骨沿骨缺损边缘向中心区域生成, 修复大部分骨缺损; 与对照组比较, BMSC-CS组大鼠颅骨骨体积分数[骨体积(BV)/组织体积(TV)]和骨小梁间距(Tb.N)均明显升高( $P<0.05$ ), CGF/BMSC-CS组大鼠颅骨BV、BV/TV、骨小梁数目(Tb.Th)和Tb.N均明显升高( $P<0.05$ ); 与BMSC-CS组比较, CGF/BMSC-CS组大鼠颅骨BV、BV/TV、Tb.Th和Tb.N均明显升高( $P<0.01$ )。HE和Masson染色观察, 对照组大鼠颅骨缺损组织几乎无新骨生成, 仅见大量胶原纤维连接两侧骨断端; BMSC-CS组大鼠颅骨缺损组织仅在骨缺损边缘有少量新骨形成, 中央为致密的胶原纤维与缺损边缘的新生骨连接;

[收稿日期] 2023-12-28

[基金项目] 吉林省财政厅医疗卫生人才建设项目(JCSZ2023481-30)

[作者简介] 石剑虹(1997-), 女, 山西省朔州市人, 在读硕士研究生, 主要从事口腔正颌和口腔颌面外科方面的研究。

[通信作者] 吴国民, 教授, 主任医师, 博士研究生导师(E-mail: guominwu2006@sina.com)

CGF/BMSC-CS组大鼠颅骨缺损组织除在骨缺损边缘可以看到新生骨组织外, 缺损中央亦有骨岛形成, 骨岛周围可见骨细胞及大量的胶原纤维。Masson染色观察, 细胞质和类骨质呈红色, 胶原呈蓝色; CGF/BMSC-CS组大鼠颅骨缺损组织中可见明显的新形成的类骨质, 新骨形成量最高。**结论:** CGF可以促进BMSCs膜片的成骨分化和ECM的丰富度, 含CGF复合CS可以高效修复大鼠颅骨缺损, 是一种理想和安全的促骨再生材料。

[关键词] 浓缩生长因子; 细胞膜片; 骨髓间充质干细胞; 骨缺损再生修复

[中图分类号] R78 [文献标志码] A

## Biological properties of concentrated growth factor combined with bone marrow mesenchymal stem cell sheet and its effect on bone defect repairment

SHI Jianhong<sup>1,2</sup>, TIAN Yuanye<sup>1</sup>, CHEN Kai<sup>1</sup>, SUN Gao<sup>1</sup>, WU Guomin<sup>1</sup>

(1. Department of Oral and Maxillofacial Surgery and oral Plastic Surgery, Stomatology Hospital, Jilin University, Changchun 130021, China; 2. Jilin Provincial Key Laboratory of Tooth Development and Bone Remodeling and Regeneration, Stomatology Hospital, Jilin University, Changchun 130021, China)

**ABSTRACT Objective:** To discuss the effect of concentrated growth factor (CGF) on the performance of bone marrow mesenchymal stem cells (BMSCs) sheets, and to clarify the role of CGF-containing composite cell sheets (CS) in the bone defect repairment. **Methods:** In *in vitro* experiments, the BMSCs were isolated and cultured from two 3-week-old SD rats; Alizarin Red S and Oil Red O staining were used to identify the osteogenic and adipogenic capabilities of BMSCs; CGF liquid extracts (CGFe) was prepared from three 3-week-old SD rats. The cells were divided into control group, traditional CS (BMSC-CS) group, and CGF-containing composite CS (CGF/BMSC-CS) group. The morphology of the CS in two groups was observed by HE staining. Alizarin Red and alkaline phosphatase (ALP) staining were used to detect the osteogenic differentiation of the CS in various groups; cell scratch assay was used to detect the migration abilities of the cells in various groups; real-time fluorescence quantitative PCR (RT-qPCR) method was used to detect the mRNA expression levels of ALP, collagen type 1 (COL-1), Runt-related transcription factor 2 (RUNX2), and osteocalcin (OCN) in the cells in various groups. In *in vivo* experiments, 15 SD rats were randomly divided into control group, BMSC-CS group, and CGF/BMSC-CS group; micro computed tomography (Micro-CT) was used to detect the bone formation parameters in skull defects of the rats in various groups; HE staining and Masson staining were used to observe the morphology of skull defect tissue of the rats in various groups. **Results:** The third-generation BMSCs were spindle-shaped, closely arranged, and grew in a vortex cluster. The Alizarin red staining results showed obvious calcium nodules, and the Oil red O staining showed red lipid droplets, confirming the cells' ability to undergo osteogenic and adipogenic differentiation. The CS were white and semi-transparent, with slightly curled edges. The peeled CS were irregularly curled and wrinkled. Compared with BMSC-CS group, the CS in CGF/BMSC-CS group were whiter, less transparent, significantly increased in thickness and extensibility, less prone to breakage, and had a certain degree of stickiness and plasticity. The HE staining results showed that compared with BMSC-CS group, the number of the cells of CS in CGF/BMSC-CS group was increased, with denser arrangement and more abundant extracellular matrix (ECM), which wrapped and connected the cells to form an integral sheet-like structure. The Alizarin red and ALP staining results showed that compared with control group, the ALP activity and mineralization uplift value of CS in BMSC-CS group were

significantly increased ( $P < 0.05$ ); compared with control group and BMSC-CS group, the number of osteoblasts and red mineralized nodules in the CS in CGF/BMSC-CS group was significantly increased, with obvious deepening of the staining, increased positive area, and the ALP activity and mineralization uplift value were significantly increased ( $P < 0.05$ ). Compared with BMSC-CS group, the ALP activity and mineralization uplift value of the CS in CGF/BMSC-CS group were increased ( $P < 0.05$ ). The cell scratch assay results showed that after 24 h of culture, compared with control group, the migration rates of the cells in BMSC-CS group and CGF/BMSC-CS group were significantly increased ( $P < 0.05$ ). Compared with BMSC-CS group, the migration rate of the cells in CGF/BMSC-CS group was significantly increased ( $P < 0.01$ ). After 48 h of culture, compared with control group, the migration rate of the cells in CGF/BMSC-CS group was significantly increased ( $P < 0.05$ ). The RT-qPCR results showed that compared with control group, the expression levels of COL-1 and OCN mRNA in the cells in BMSC-CS group were significantly increased ( $P < 0.01$ ), and the expression levels of ALP, COL-1, OCN, and RUNX2 mRNA in the cells in CGF/BMSC-CS group were significantly increased ( $P < 0.01$ ). Compared with BMSC-CS group, the expression levels of ALP, COL-1, and OCN mRNA in the cells in CGF/BMSC-CS group were significantly increased ( $P < 0.01$ ). The Micro-CT detection results showed that in control group, the boundary of the rat skull defect area was clear, with almost no new bone formation. In BMSC-CS group, a small amount of new bone formed only at the edge of the bone defect in skull of the rats, with a significant gap in the central area of the defect. In CGF/BMSC-CS group, new bone formed along the edge of the bone defect towards the central area in skull of the rats, repairing most of the bone defect. Compared with control group, the bone volume (BV) and trabecular number (Tb.N) of the rats in BMSC-CS group were significantly increased ( $P < 0.05$ ); the bone volume (BV), bone volume fraction [BV/tissue volume (TV)], trabecular thickness (Tb.Th), and trabecular number (Tb.N) in skull of the rats in CGF/BMSC-CS group, were significantly increased ( $P < 0.05$ ). Compared with BMSC-CS group, the BV, BV/TV, Tb.Th, and Tb.N in skull of the rats in CGF/BMSC-CS group were significantly increased ( $P < 0.01$ ). The HE and Masson staining observation showed that in control group, almost no new bone formed in the skull defect tissue of the rats, with only a large amount of collagen fibers connecting the two sides of the bone ends. In BMSC-CS group, a small amount of new bone formed only at the edge of the bone defect in skull tissue of the rats, with the central area of the defect containing dense collagen fibers connected to the newly formed bone at the defect edge. In CGF/BMSC-CS group, new bone tissue could be seen at the edge of the bone defect, and bone islands formed in the central area of the defect, surrounded by osteocytes and a large amount of collagen fibers. The Masson staining observation results showed that the cytoplasm and osteoid were red, and the collagen was blue. In CGF/BMSC-CS group, newly formed osteoid was observed in skull defect tissue of the rats, with the highest amount of new bone formation. **Conclusion:** CGF can promote the osteogenic differentiation and increase the richness of ECM in BMSCs sheets. CGF-containing composite CS can efficiently repair skull defects of the rats and serve as an ideal and safe material for promoting the bone regeneration.

**KEYWORDS** Concentrated growth factor; Cell sheet; Bone marrow mesenchymal stem cell; Bone defect regeneration and repairment

近年来, 细胞膜片 (cell sheet, CS) 技术被广泛应用于骨缺损的再生修复, 其克服了传统细胞用于组织工程时的缺点, 如胰酶消化造成的细胞外基质和细胞间连接蛋白减少、细胞存活率低及细胞活性不足等<sup>[1]</sup>。CS 包含大量种子细胞和细胞外基质 (extracellular matrix, ECM), ECM 作为

内源性支架可以增加细胞生物活性, 其紧密的片状结构使细胞保存状态完好, 细胞存活率高且分布均匀, 具有较好的黏附和增殖能力, 从而提高了修复骨缺损的能力。目前, CS 技术已被用于修复关节软骨、骨、牙周韧带、角膜、血管和心肌的损伤<sup>[2-3]</sup>。骨髓间充质干细胞 (bone marrow mesenchymal stem

cells, BMSCs) 因其易获得性、增殖能力强和成骨分化效果好等优点, 是最常用的种子细胞之一。AKAHANE等<sup>[4]</sup>成功构建大鼠BMSCs膜片, 植入大鼠皮下部位6周后, 在移植处发现矿化基质和活跃的成骨细胞, 证实CS的成骨性能良好。

生长因子在骨缺损再生中起着关键作用, 将生长因子或小分子物质复合至膜片中可以提高其成骨能力。QI等<sup>[5]</sup>将富血小板血浆(platelet-rich plasma, PRP)/磷酸钙(calcium phosphate, CaP)复合物作用于CS, 证实其具有更强的促进骨缺损修复的能力。浓缩生长因子(concentrated growth factor, CGF)是继PRP和富血小板纤维蛋白(platelet rich fibrin, PRF)之后第三代血小板浓缩物, 是富含高浓度生长因子的自体纤维蛋白支架, 有利于干细胞的附着<sup>[6]</sup>。CGF可通过变速离心法制备, 避免血液中的生长因子受到破坏并完全分离血液中的各种细胞成分, 因此能够获得浓度极高的各种生长因子, 主要包括转化生长因子 $\beta 1$ (transforming growth factor- $\beta 1$ , TGF- $\beta 1$ )、表皮生长因子(epidermal growth factor, EGF)、骨形态发生蛋白(bone morphogenetic proteins, BMPs)、血管内皮生长因子(vascular endothelial growth factor, VEGF)和胰岛素样生长因子1(insulin like growth factor-1, IGF-1)等, 相关内源性生长因子具有协同效应和级联效应, 明显影响细胞的增殖、分化和迁移<sup>[7-8]</sup>。本研究通过维生素C诱导BMSCs形成CS, 即传统CS(BMSC-CS), 同时在成膜诱导过程中加入CGF, 构建复合CS(CGF/BMSC-CS), 分析2种CS的细胞活性、组织结构和体内外成骨能力, 探讨CGF对BMSCs膜片生物学性能的影响, 并阐明其在骨缺损再生修复应用中的潜能。

## 1 材料与方法

**1.1 实验动物、主要试剂和仪器** 5只2~3周龄SD大鼠, 体质量50~100 g, 15只7~8周龄SD大鼠, 体质量200~250 g, 购自长春亿斯实验动物技术有限责任公司, 实验动物使用许可证号: SYXK(吉)2023-0010。实验动物饲养于吉林大学基础医学院动物房中, 环境清洁, 恒温恒湿, 定期消毒和通风, 实验前所有大鼠适应性喂养1周。本研究经过吉林大学基础医学院动物伦理委员会批准(伦理审批号: 2022450), 实验过程均符合实验室动物伦理准则。胎牛血清(fetal bovine serum, FBS)购自杭州四季青公司, 磷酸盐缓冲液(phosphate

buffered saline, PBS)购自美国Gibco公司,  $\alpha$ -MEM培养基和DMEM高糖培养基购自美国HyClone公司, 抗坏血酸购自美国Sigma公司, TRIzol裂解液购自日本TaKaRa公司。CGF变速离心机购自北京创英科技有限公司, 超净工作台购自日本AIRTECH公司, PCR仪购自瑞士Roche公司。

**1.2 大鼠BMSCs分离、培养和鉴定** 取2只3周龄SD大鼠, 颈椎脱臼法处死, 75%乙醇溶液浸泡10 min。剥去皮毛, 取双侧股骨和胫骨, 于超净台上剪除两端骨骺端, 用1 mL无菌注射器吸取含1%双抗和10% FBS的 $\alpha$ -MEM培养基, 反复冲洗3次, 直至骨髓腔变白, 收集骨髓冲出液, 反复敲打使骨髓组织均匀分布。于37℃、5% CO<sub>2</sub>和100%饱和湿度环境细胞培养箱中静置培养, 培养48 h待细胞贴壁完全后首次换液, 以后每2~3 d换液。约6~8 d后细胞生长至培养皿80%~90%, 进行传代培养。取第3代BMSCs, 以 $2 \times 10^6$  mL<sup>-1</sup>的细胞密度接种于6孔细胞培养板中, 含10% FBS的 $\alpha$ -MEM培养基培养, 至细胞生长至80%融合时, 将培养基更换为含50 mg·L<sup>-1</sup>维生素C、10 mmol·L<sup>-1</sup>  $\beta$ -甘油磷酸钠、10 nmol·L<sup>-1</sup>地塞米松和10% FBS的DMEM高糖培养基成骨诱导液, 成骨诱导21 d后, PBS缓冲液冲洗, 4%多聚甲醛溶液固定30 min, 1%茜素红染液染色3~5 min, 倒置显微镜下观察细胞成骨情况并拍照。更换成脂诱导液, 诱导3周, PBS缓冲液冲洗, 4%多聚甲醛溶液固定30 min, 油红O染色3~5 min, 倒置显微镜下观察脂滴形成情况并拍照。

**1.3 CGF液态提取物(CGF liquid extracts, CGFe)制备** 3只3周龄SD大鼠, 1%戊巴比妥钠麻醉, 腹主静脉采血并置于变速离心机内离心, 加速30 s, 2 700 r·min<sup>-1</sup>、2 min; 2 400 r·min<sup>-1</sup>、4 min; 2 700 r·min<sup>-1</sup>、4 min; 3 000 r·min<sup>-1</sup>、3 min, 减速36 s后停止。离心后血液样本分为3层, 上层为PRP, 中层为富含生长因子的淡黄色凝胶样CGF, 下层为红细胞(red blood cell, RBC)层。剪取中间凝胶层, PBS缓冲液冲洗, -80℃冷冻1 h, 解冻后于4℃下, 230 g离心5 min, 然后加入5 mL  $\alpha$ -MEM培养基, 37℃孵育24 h, 400 g离心5 min。收集5 mL上清液, 0.22  $\mu$ m过滤器过滤, 作为CGFe<sup>[9]</sup>。根据HONDA等<sup>[10]</sup>的研究方法, 选择促进BMSCs成骨分化的最佳浓度10% CGFe进行后续实验。

**1.4 细胞分组和培养** 选择第3代BMSCs, 以 $2 \times 10^6 \text{ mL}^{-1}$ 的细胞密度接种于6孔细胞培养板中。将细胞分为对照组、BMSC-CS组和CGF/BMSC-CS组。待细胞密度达到70%~80%时, 对照组仅用高糖DMEM培养基培养, BMSC-CS组更换为含 $100 \text{ mg} \cdot \text{L}^{-1}$ 维生素C和10% FBS的高糖DMEM培养基成膜诱导液, CGF/BMSC-CS组加入含10%CGF的成膜诱导液, 每2~3 d换液, 连续培养14 d, 孔底可见白色膜片形成, 用细胞刮刀小心获取完整膜片用于后续实验。

**1.5 HE染色观察2组CS形态表现** CS成熟后, 吸弃培养液, 获取完整膜片, PBS缓冲液冲洗3次, 4%多聚甲醛固定4 h, PBS缓冲液再次冲洗3次, 扫描记录其大体形态。随后常规脱水, 石蜡包埋, 组织学切片, HE染色, 于光学显微镜下观察2组CS形态表现并记录。

**1.6 茜素红和碱性磷酸酶(alkaline phosphatase, ALP)染色检测各组CS体外成骨情况** 获取CS, PBS缓冲液冲洗3次, 4%多聚甲醛固定30 min, PBS缓冲液再次冲洗3次, 分别进行茜素红和ALP染色, 显微镜下观察各组CS体外成骨情况, 采用Image J软件分析吸光度(A)值, 计算各组CS矿化提升值和ALP活性。矿化提升值=茜素红染色实验孔A值/茜素红染色对照孔A值; ALP活性=ALP染色实验孔A值/ALP染色对照孔A值。

**1.7 细胞划痕实验检测各组细胞迁移能力** 在6孔细胞培养板底部等间距画出3条平行直线, 将P3代BMSCs消化后, 均匀接种至6孔细胞培养板, 每孔 $5 \times 10^5$ 个, 置于细胞培养箱内培养; 当细胞长满孔底时, 用 $200 \mu\text{L}$ 灭菌枪头沿标记划直线, PBS缓冲液小心冲洗后更换为成膜培养基, 0、24和48 h后观察拍照, 采用Image J软件检测细胞迁移面积, 计算各组细胞迁移率, 代表各组细胞迁移能力。细胞迁移率=(0 h划痕面积-24 h或48 h划痕面积)/0 h划痕面积 $\times 100\%$ 。

**1.8 实时荧光定量PCR(real-time fluorescence quantitative PCR, RT-qPCR)法检测各组细胞中ALP、胶原酶I型(collegenase type 1, COL-1)、Runt相关转录因子2(runt-related transcription factor 2, RUNX2)和骨钙蛋白(osteocalcin, OCN)mRNA表达水平** 分别提取各组细胞总RNA, DEPC水溶解, Nanodrop测定RNA浓度, 逆转录

为cDNA, SYBR法扩增, 以GAPDH作为内参, 采用 $2^{-\Delta\Delta C_t}$ 法计算各组细胞中成骨相关因子ALP、COL-1、RUNX2和OCN mRNA表达水平, 至少3次独立重复实验。引物序列见表1。

表1 成骨相关基因引物序列

Tab. 1 Primer sequences of osteogenic related gene

Gene	Primer sequence
GAPDH	F 5'-AAGTTCAACGGCAGTCAAGG-3' R 5'-GACATACTCAGCACCAGCATCAC-3'
ALP	F 5'-AGACTCTCAGGAGGCATAGACTTC-3' R 5'-GCACAGGTTGGCGGCTTC-3'
RUNX2	F 5'-TCGTCAGCGTCCTATCAGTTCCR-3' R 5'-CTTCCATCAGCGTCAACACCATC-3'
OCN	F 5'-GACCCTCTCTGCTCACTCTG-3' R 5'-CACCACCTTACTGCCCTCCTG-3'
COL-1	F 5'-TGGTCCTGCTGGCAAGAATGG-3' R 5'-TCTGTCACCTTGTTGCCTGTG-3'

**1.9 大鼠颅骨缺损模型制备和膜片植入** 15只7~8周龄SPF级雄性SD大鼠, 体质量( $250 \pm 25$ )g, 随机分为对照组、BMSC-CS组和CGF/BMSC-CS组, 每组5只。清洁环境饲养, 自由进食和饮水, 定期环境消毒。腹腔注射2%戊巴比妥麻醉大鼠, 仰卧位固定大鼠四肢, 脱去头部毛发, 消毒头皮部位, 铺巾完毕, 在无菌条件下利用手术刀片沿颅中缝作长约2 cm的纵形切口, 切开皮肤、皮下组织、肌层和骨膜层, 钝性分离暴露颅骨骨板, 建造全层圆形缺损, 不损伤硬脑膜。用外科电动空心环钻于颅骨制备直径为5 mm、厚度为1 mm的全层圆形骨缺损, 操作过程中利用生理盐水持续冲洗。对照组大鼠不放置任何材料, 其余2组大鼠放置等量BMSC-CS和CGF/BMSC-CS, 填充整个圆形骨缺损区, 对位缝合伤口。

**1.10 显微计算机断层扫描(micro-computed tomography, Micro-CT)检测各组大鼠颅骨缺损处骨形成参数** 术后6周处死大鼠, 10%多聚甲醛固定48 h。进行Micro-CT扫描, 三维重建。选择所制备的5 mm $\times$ 1 mm颅骨缺损区为感兴趣区域(region of interest, ROI)进行扫描, 获取各组大鼠颅骨骨体积(bone volume, BV)、骨体积分数[BV/组织体积(tissue volume, TV)]、骨小梁数目(trabecular number, Tb. N)和骨小梁间距(trabecular thickness, Tb. Th)。

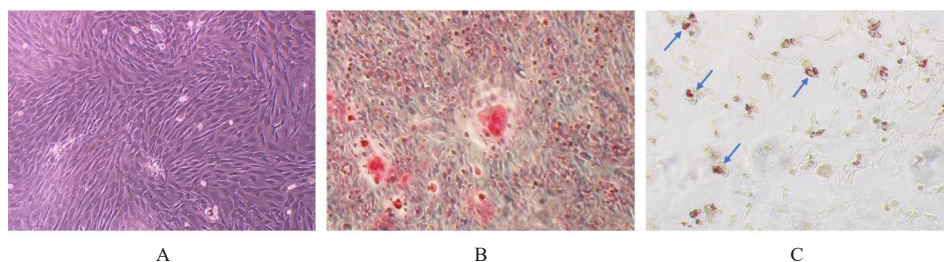
**1.11 HE染色和Masson染色观察各组大鼠颅骨缺损组织形态表现** 将大鼠颅骨标本使用EDTA脱钙50 d, 石蜡包埋, 制备成5  $\mu\text{m}$ 厚的切片。HE染色, 光学显微镜下观察并采集图像, 观察新生骨组织形态表现。Masson染色, 切片按照Masson染液套装说明书进行操作, 封片, 倒置相差显微镜下观察骨组织形态表现并采集图像。

**1.12 统计学分析** 采用GraphPad Prism 9.0统计软件进行统计学分析。各组CS矿化提升值和ALP活性, 各组细胞迁移率和BMSC-CS及CGF/BMSC-CS成骨相关基因mRNA表达水平, 各组大鼠颅骨缺

损处骨形成参数均符合正态分布, 以 $\bar{x}\pm s$ 表示, 多组间样本均数比较采用单因素方差分析, 组间样本均数两两比较采用Student's *t*检验。以 $P<0.05$ 为差异有统计学意义。

## 2 结果

**2.1 大鼠BMSCs鉴定** 倒置显微镜下可见第3代BMSCs为梭形, 排列紧密, 呈漩涡团簇状生长; 茜素红染色有明显的钙结节生成, 油红O染色有红色脂滴形成, 证实细胞具有良好的成骨和成脂分化的能力。见图1。



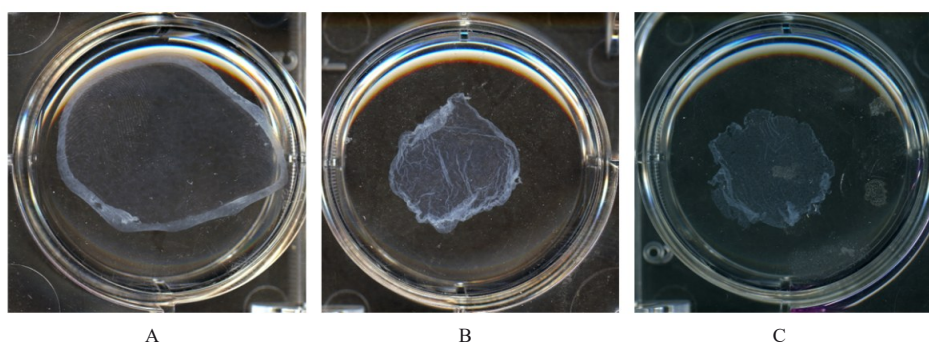
A: Third generation cells( $\times 4$ ); B: Alizarin red staining( $\times 4$ ); C: Oil red O staining(Arrows showed red lipid droplets,  $\times 10$ )

图1 BMSCs的鉴定

Fig. 1 Identification of BMSCs

**2.2 2组CS形态表现** CS为白色半透明状, 边缘轻微卷曲, 剥离后的CS卷曲皱缩为不规则状。与BMSC-CS组比较, CGF/BMSC-CS组CS白色更深, 透明程度较低, 在厚度和延展性方面明显增

加, 不易破损, 有一定黏性和可塑性。HE染色结果显示: 与BMSC-CS组比较, CGF/BMSC-CS组CS细胞数增加, 排列密集, ECM更丰富, 包裹连接细胞形成一个整体的片状结构。见图2和3。



A: Edge of cell sheet; B: Gross observation of CGF/BMSC-CS; C: Gross observation of BMSC-CS.

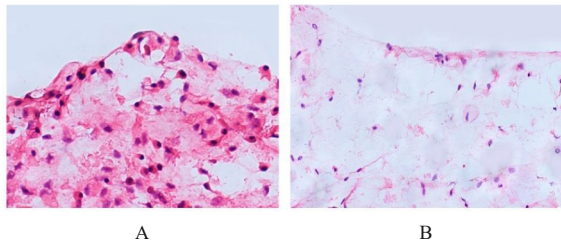
图2 2组CS大体形态

Fig. 2 Gross morphology of CS in two groups

**2.3 各组CS体外成骨情况** 与对照组比较, BMSC-CS组CS的ALP活性和矿化提升值均明显升高( $P<0.05$ )。与对照组和BMSC-CS组比较, CGF/BMSC-CS组CS的成骨细胞及红色矿化结节

数明显增多, 染色明显加深, 阳性面积增大, ALP活性和矿化提升值均明显升高( $P<0.05$ )。见图4~7和表2。

**2.4 各组细胞迁移率** 培养24 h, 与对照组比较,

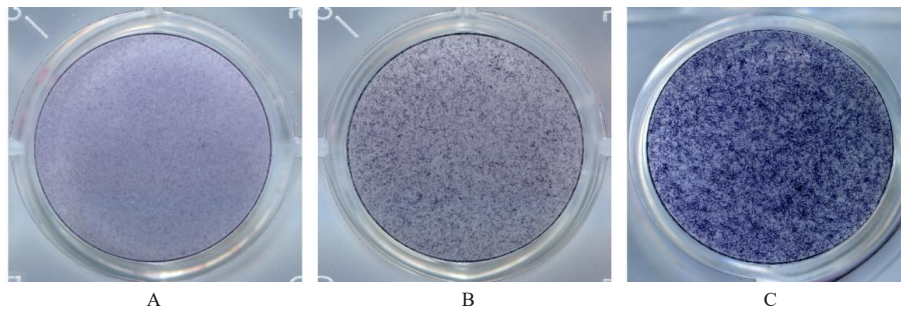


A: CGF/BMSC-CS group; B: BMSC-CS group.

图3 HE染色观察2组CS形态表现( $\times 20$ )

Fig. 3 Morphology of CS in two groups observed by HE staining( $\times 20$ )

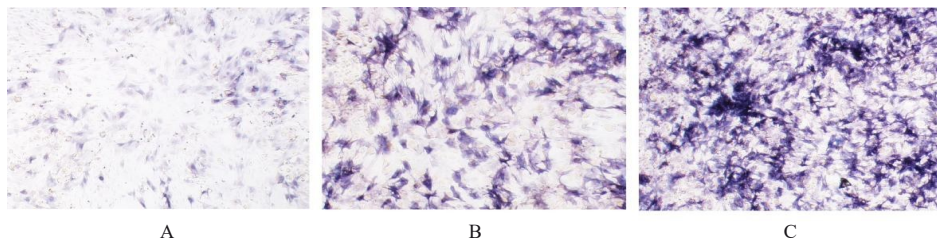
BMSC-CS组和CGF/BMSC-CS组细胞迁移率均明显升高 ( $P < 0.05$ ); 与BMSC-CS组比较, CGF/BMSC-CS组细胞迁移率明显升高 ( $P < 0.01$ )。培养48 h, 与对照组比较, BMSC-CS组细胞迁移率升高, 但差异无统计学意义 ( $P > 0.05$ ), CGF/BMSC-CS组细胞迁移率明显升高 ( $P < 0.05$ ); 与BMSC-CS组比较, CGF/BMSC-CS组细胞迁移率升高, 但差异无统计学意义 ( $P > 0.05$ )。见图8和表3。



A: Control group; B: BMSC-CS group; C: CGF/BMSC-CS group.

图4 ALP染色观察各组CS大体形态表现

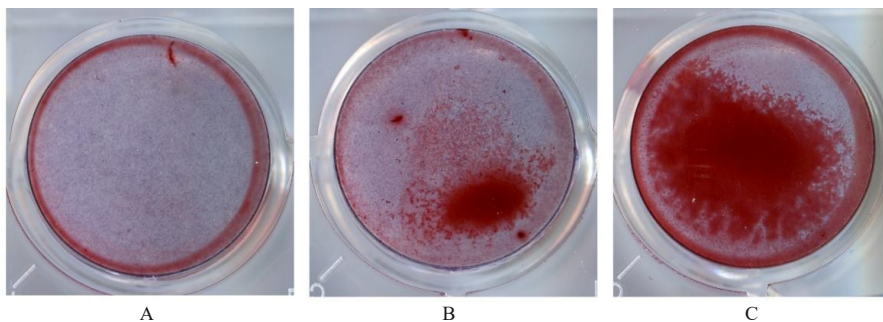
Fig. 4 Gross morphology of CS in various groups observed by ALP staining



A: Control group; B: BMSC-CS group; C: CGF/BMSC-CS group.

图5 ALP染色观察各组CS形态表现( $\times 4$ )

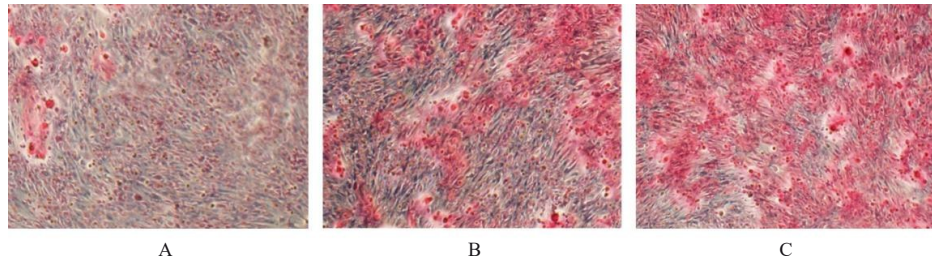
Fig. 5 Morphology of CS in various groups observed by ALP staining( $\times 4$ )



A: Control group; B: BMSC-CS group; C: CGF/BMSC-CS group.

图6 茜素红染色观察各组CS大体形态表现

Fig. 6 Gross morphology of CS in various groups observed by Alizarin red staining



A: Control group; B: BMSC-CS group; C: CGF/BMSC-CS group.

图7 茜素红染色观察各组CS形态表现(×4)

Fig. 7 Morphology of CS in various groups observed by Alizarin red staining(×4)

表2 各组CS的ALP活性和矿化提升值

Tab. 2 Activities of ALP and mineralisation uplift values of CS in various groups (n=3,  $\bar{x} \pm s$ )

Group	Activity of ALP	Mineralisation uplift value
Control	1.00±0.02	1.00±0.06
BMSC-CS	1.14±0.03*	1.37±0.05*
CGF/BMSC-CS	1.42±0.10 <sup>△</sup>	2.00±0.17 <sup>△</sup>

\*P<0.05 compared with control group; <sup>△</sup>P<0.05 compared with BMSC-CS group.

2.5 各组细胞中ALP、COL-1、Runx2和OCN mRNA表达水平 与对照组比较, BMSC-CS组细胞中COL-1和OCN mRNA表达水平均明显升高 (P<0.01), ALP和RUNX-2 mRNA表达水

平升高, 但差异均无统计学意义 (P>0.05); CGF/BMSC-CS组细胞中ALP、COL-1、OCN和RUNX-2 mRNA表达水平均明显升高 (P<0.01)。与BMSC-CS组比较, CGF/BMSC-CS组细胞中ALP、COL-1和OCN mRNA表达水平均明显升高 (P<0.01), RUNX-2 mRNA表达水平升高, 但差异无统计学意义 (P>0.05)。见表4。

2.6 各组大鼠颅骨缺损处骨形成参数 对照组大鼠颅骨缺损区域边界清晰, 几乎无新骨生成; BMSC-CS组大鼠颅骨仅在骨缺损边缘有少量新骨形成, 缺损中心区域有明显空缺; CGF/BMSC-CS组大鼠颅骨新骨沿骨缺损边缘向中心区域生成,

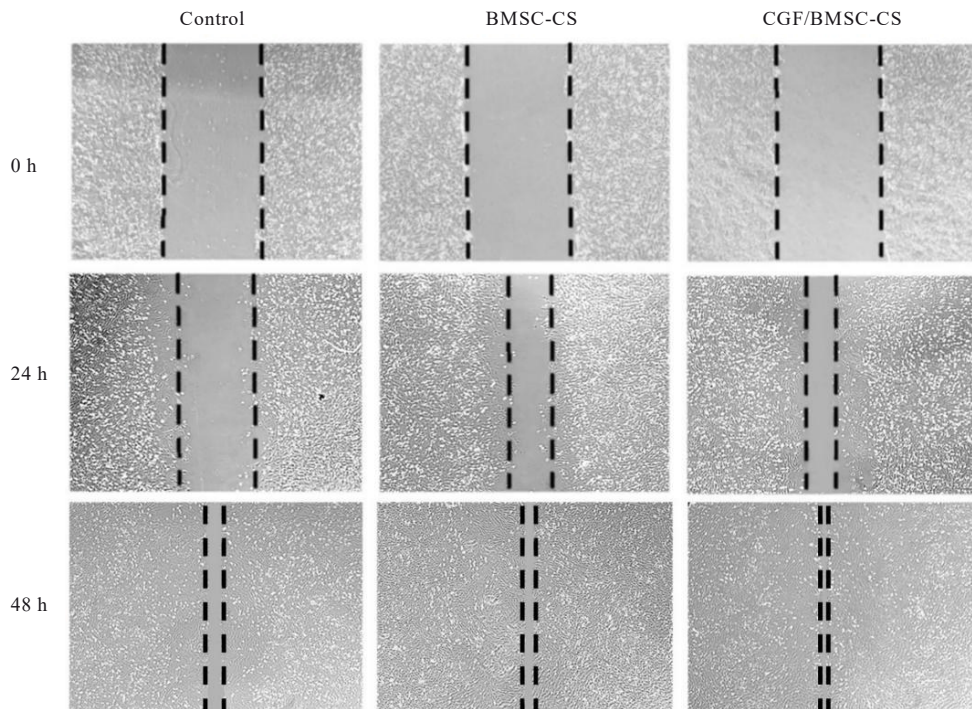


图8 各组细胞迁移情况(×4)

Fig. 8 Migration of cells in various groups(×4)

表3 各组细胞迁移率

Tab. 3 Migration rates of cells in various groups  
( $n=3, \bar{x} \pm s, \eta/\%$ )

Group	Migration rate		
	(t/h)	24	48
Control		19.29±1.40	91.56±2.00
BMSC-CS		36.90±1.94*	95.39±1.28
CGF/BMSC-CS		47.61±3.15* <sup>△</sup>	96.84±1.56*

\* $P<0.05$  compared with control group; <sup>△</sup> $P<0.01$  compared with BMSC-CS group.

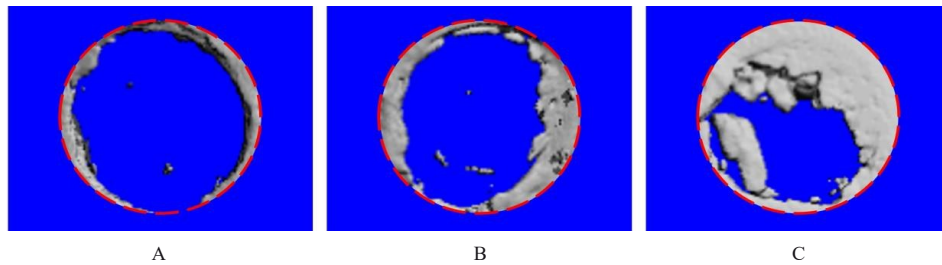
修复大部分骨缺损。与对照组比较, BMSC-CS组大鼠颅骨BV/TV和Tb.N均明显升高( $P<0.05$ ), BV和Tb.Th升高, 但差异无统计学意义( $P>0.05$ ), CGF/BMSC-CS组大鼠颅骨BV、BV/TV、Tb.Th和Tb.N均明显升高( $P<0.05$ )。与BMSC-CS组比较, CGF/BMSC-CS组大鼠颅骨BV、BV/TV、Tb.Th和Tb.N均明显升高( $P<0.01$ )。见图9和表5。

表4 各组细胞中成骨相关基因 mRNA 表达水平

Tab. 4 Expression levels of osteogenic-related genes mRNA in cells in various groups ( $n=3, \bar{x} \pm s$ )

Group	ALP	COL-1	RUNX-2	OCN
Control	1.00±0.11	1.00±0.07	1.00±0.11	1.00±0.10
BMSC-CS	1.09±0.17	1.25±0.06*	1.07±0.11	1.23±0.16*
CGF/BMSC-CS	2.82±0.67* <sup>△</sup>	1.81±0.19* <sup>△</sup>	1.21±0.12*	1.77±0.23* <sup>△</sup>

\* $P<0.01$  compared with control group; <sup>△</sup> $P<0.01$  compared with BMSC-CS group.



Red circle represented margin of skull defect. A: Control group; B: BMSC-CS group; C: CGF/BMSC-CS group.

图9 各组大鼠颅骨缺损处骨形成情况(×6)

Fig. 9 Bone formations at cranial defects of rats in various groups(×6)

表5 各组大鼠颅骨缺损处骨形成参数

Tab. 5 Parameters of bone formation at cranial defects of rats in various groups ( $n=3, \bar{x} \pm s$ )

Group	BV( $V/mm^3$ )	BV/TV( $\eta/\%$ )	Tb.Th( $l/mm$ )	Tb.N( $l/mm$ )
Control	0.20±0.08	2.09±1.06	0.15±0.04	0.13±0.05
BMSC-CS	3.11±0.95	11.71±2.80*	0.17±0.04	0.70±0.09*
CGF/BMSC-CS	17.23±1.20* <sup>△</sup>	35.80±1.81* <sup>△</sup>	0.53±0.02* <sup>△</sup>	1.16±0.03* <sup>△</sup>

\* $P<0.05$  compared with control group; <sup>△</sup> $P<0.01$  compared with BMSC-CS group.

2.7 各组大鼠颅骨缺损组织形态表现 选取骨缺损边缘略靠近中间部位进行放大, 两侧为骨缺损边缘, 中心为骨缺损区域。HE染色观察可见, 对照组大鼠颅骨缺损组织几乎无新骨生成, 仅见大量胶原纤维连接两侧骨断端; BMSC-CS组大鼠颅骨缺损组织仅在骨缺损边缘有少量新骨形成, 中央为致密的胶原纤维与缺损边缘的新生骨连接;

CGF/BMSC-CS组大鼠颅骨缺损组织除在骨缺损边缘可以看到新生骨组织外, 缺损中央亦有骨岛形成, 骨岛周围可见骨细胞及大量的胶原纤维。Masson染色可见细胞质和类骨质呈红色, 胶原呈蓝色。CGF/BMSC-CS组大鼠颅骨缺损组织中可见明显的新形成的类骨质, 新骨形成量最高。见图10和11。

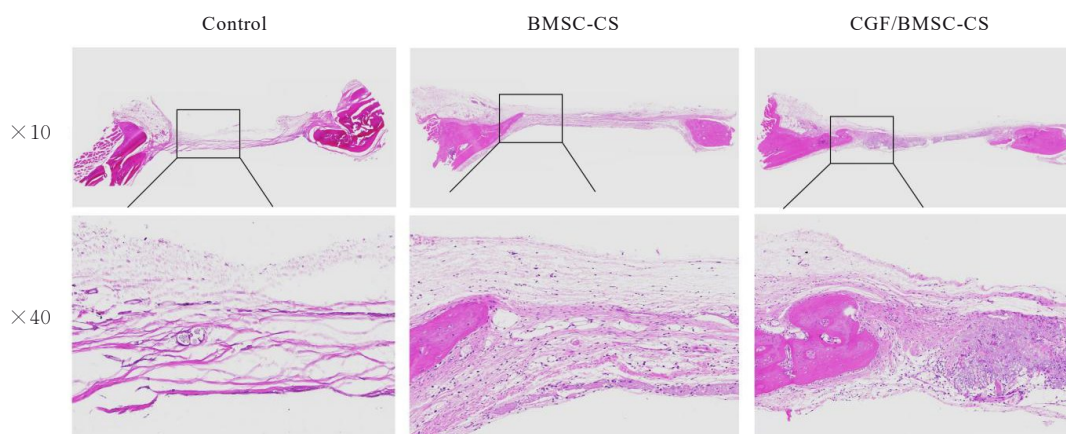
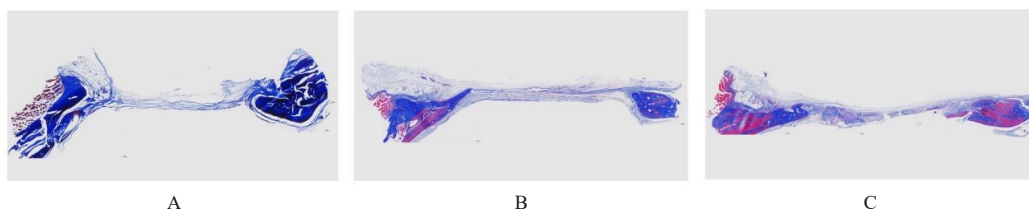


图10 HE染色观察各组大鼠颅骨缺损组织形态表现

Fig. 10 Morphology of cranial defects of rats in various groups observed by HE staining



A: Control group; B: BMSC-CS group; C: CGF/BMSC-CS group.

图11 Masson染色观察各组大鼠颅骨缺损组织形态表现( $\times 10$ )

Fig. 11 Morphology of cranial defects of rats in various groups observed by Masson staining ( $\times 10$ )

### 3 讨论

CS是一种新型培养和获取细胞的方法,而机械法是目前制备干细胞膜片最简单的一种方法<sup>[2, 11]</sup>。CS可以保留一个相对完整的ECM,从而通过旁分泌作用促进周围细胞的生长和增殖<sup>[12]</sup>。同时ECM储存了大量生长因子和功能性蛋白,参与细胞与细胞和细胞与组织之间的信号传递,提供并维持细胞微环境,对细胞功能至关重要。CS是一种具有发展前景的基于细胞的治疗方法,在骨组织修复中发挥关键作用<sup>[13-14]</sup>。然而,传统的细胞膜片存在细胞分化能力不足、可塑性差和成骨能力欠缺等缺点,尤其是由于缺乏可靠的血液供应,无法满足大面积骨缺损的再生修复<sup>[15-16]</sup>。因此,提高CS的均匀性,促进微血管网络的形成和ECM的发展是CS制备的主要目标<sup>[17-18]</sup>。

研究<sup>[19]</sup>显示:10% CGF能明显促进BMSCs的增殖和成骨分化。本研究采用10% CGFe作用于细胞,促进BMSCs增殖、成骨向分化和ECM分泌,弥补传统CS的不足。本研究结果显示:与BMSC-CS组比较,CGF/BMSC-CS组CS在韧性

及厚度方面更有优势,方便获取紧密连接的完整膜片,含有更多数量的细胞,ECM更加丰富,加强了细胞与细胞的连接及信号通路作用。同时丰富的ECM包裹细胞连成一个整体结构,为细胞的生长、增殖和分化提供良好的支架,有利于细胞与细胞之间的相互作用。

ALP作为成骨细胞分化的标志物,最先出现于细胞矿化的早期阶段,可作为早期成骨标志物,钙盐水平代表了骨细胞增殖、分化和骨组织的成骨潜能,因此采用ALP染色和茜素红染色分别评价早期和晚期成骨作用<sup>[19-20]</sup>。本研究中茜素红和ALP染色结果显示:CGF/BMSC-CS组成骨细胞及钙化结节数最多,提示其成骨能力较强。与BMSC-CS组比较,CGF/BMSC-CS组ALP活性和矿化提升值明显升高,提示CGF在整个成骨过程中均促进了BMSCs的成骨分化,维持了成骨诱导的连续性。细胞划痕实验结果显示:CGF可以有效促进BMSCs的增殖和迁移,提高细胞的再生修复作用。CGF/BMSC-CS通过上调成骨相关基因ALP、COL-1、OCN和RUNX-2 mRNA表达,促进BMSCs的增殖和成骨分化,其中对ALP的上调作

用最为明显,可能是由于丰富的ECM提供了良好的成骨微环境。

三维重建图和HE及Masson染色结果显示:CGF/BMSC-CS组大鼠颅骨缺损处新骨不仅沿骨缺损边缘形成,同时在缺损中心区域也有新骨单独形成。一般情况下,诱导骨形成的细胞主要来源于骨缺损区的边缘,新骨主要从骨缺损周围逐渐向中心发展<sup>[21]</sup>。本研究结果显示:CGF/BMSC-CS组大鼠颅骨缺损处形成了不与缺损边缘相连的新骨,提示CGF不仅促进BMSCs的成骨向分化,同时也促进BMSCs生成新骨并促进新骨成熟。本研究结果显示:CGF/BMSC-CS组CS对新生骨形成和成熟均具有促进作用,CGF/BMSC-CS组大鼠颅骨缺损组织新生骨周围也存在新生血管,CGF中包含CD34阳性细胞及VEGF、碱性成纤维细胞生长因子(basic fibroblast growth factor, bFGF)、基质金属蛋白酶(matrix metalloproteinase, MMP)-2和MMP-9等多种血管生成生长因子,可以刺激受损血管生成,为组织再生提供足够的营养、生长因子、矿物质和氧,血液的供应有利于成骨,证实CGF具有指导骨再生和促进局部血管化的双重作用,在一定程度上弥补了传统CS因缺乏血液供应导致的骨再生能力不足<sup>[22-24]</sup>。

研究<sup>[25]</sup>显示:CGF中IGF-1可以促进软骨细胞ECM的合成。本研究结果显示:ECM丰度升高提示CGF可能通过IGF-1促进BMSCs的ECM合成;同时ECM蛋白可结合并储存CGF释放出的生长因子,调节其在细胞中的分布、激活和呈递,达到长期的效果。此相互作用可能是CGF/BMSC-CS表现出良好成骨能力的原因之一。

综上所述,CGF可以提供细胞增殖和分化所需的因子,促进ECM分泌,CGF/BMSC-CS复合膜片具有适宜的厚度,增强了可塑性,且细胞成骨向分化明显,细胞状态良好,ECM丰富,同时具备了较强的骨再生能力,是一种理想和安全的促骨再生材料。

#### 利益冲突声明:

所有作者声明不存在利益冲突。

#### 作者贡献声明:

石剑虹参与文献检索、实验设计、实验操作、数据整理和论文撰写,田原野、陈楷、孙高和吴国民参与文献检索及论文审校。

#### [参考文献]

- [1] ELLOUMI-HANNACHI I, YAMATO M, OKANO T. Cell sheet engineering: a unique nanotechnology for scaffold-free tissue reconstruction with clinical applications in regenerative medicine [J]. *J Intern Med*, 2010, 267(1): 54-70.
- [2] TAKEZAWA T, MORI Y, YOSHIKATO K. Cell culture on a thermo-responsive polymer surface [J]. *Bio/Technology*, 1990, 8: 854-856.
- [3] SEKINE H, SHIMIZU T, SAKAGUCHI K, et al. *In vitro* fabrication of functional three-dimensional tissues with perfusable blood vessels [J]. *Nat Commun*, 2013, 4: 1399.
- [4] AKAHANE M, NAKAMURA A, OHGUSHI H, et al. Osteogenic matrix sheet-cell transplantation using osteoblastic cell sheet resulted in bone formation without scaffold at an ectopic site [J]. *J Tissue Eng Regen Med*, 2008, 2(4): 196-201.
- [5] QI Y Y, ZHAO T F, YAN W Q, et al. Mesenchymal stem cell sheet transplantation combined with locally released simvastatin enhances bone formation in a rat tibia osteotomy model [J]. *Cytotherapy*, 2013, 15(1): 44-56.
- [6] HU T Q, ZHANG H, YU W, et al. The combination of concentrated growth factor and adipose-derived stem cell sheet repairs skull defects in rats [J]. *Tissue Eng Regen Med*, 2021, 18(5): 905-913.
- [7] RODELLA L F, FAVERO G, BONINSEGNA R, et al. Growth factors, CD34 positive cells, and fibrin network analysis in concentrated growth factors fraction [J]. *Microsc Res Tech*, 2011, 74(8): 772-777.
- [8] ROCHIRA A, SICULELLA L, DAMIANO F, et al. Concentrated growth factors (CGF) induce osteogenic differentiation in human bone marrow stem cells [J]. *Biology*, 2020, 9(11): 370.
- [9] ZHOU Y, LIU X Y, SHE H J, et al. A silk fibroin/chitosan/nanohydroxyapatite biomimetic bone scaffold combined with autologous concentrated growth factor promotes the proliferation and osteogenic differentiation of BMSCs and repair of critical bone defects [J]. *Regen Ther*, 2022, 21: 307-321.
- [10] HONDA H, TAMAI N, NAKA N, et al. Bone tissue engineering with bone marrow-derived stromal cells integrated with concentrated growth factor in *Rattus norvegicus* calvaria defect model [J]. *J Artif Organs*, 2013, 16(3): 305-315.
- [11] 王宇洁, 邹杰林, 蔡明轩, 等. 壳聚糖基水凝胶在口腔

- 组织工程中的应用[J]. 中南大学学报(医学版), 2023, 48(1): 138-147.
- [12] WEI X B, WANG L, DUAN C M, et al. Cardiac patches made of brown adipose-derived stem cell sheets and conductive electrospun nanofibers restore infarcted heart for ischemic myocardial infarction [J]. *Bioact Mater*, 2023, 27: 271-287.
- [13] HYNES R O. The extracellular matrix: not just pretty fibrils[J]. *Science*, 2009, 326(5957): 1216-1219.
- [14] THUMMARATI P, LAIWATTANAPAISAL W, NITTA R, et al. Recent advances in cell sheet engineering: from fabrication to clinical translation [J]. *Bioengineering*, 2023, 10(2): 211.
- [15] YOU Q, LU M X, LI Z Z, et al. Cell sheet technology as an engineering-based approach to bone regeneration [J]. *Int J Nanomedicine*, 2022, 17: 6491-6511.
- [16] KIM Y, LEE S H, KANG B J, et al. Comparison of osteogenesis between adipose-derived mesenchymal stem cells and their sheets on poly- $\epsilon$ -caprolactone/ $\beta$ -tricalcium phosphate composite scaffolds in canine bone defects[J]. *Stem Cells Int*, 2016, 2016: 8414715.
- [17] NAKAMURA A, AKAHANE M, SHIGEMATSU H, et al. Cell sheet transplantation of cultured mesenchymal stem cells enhances bone formation in a rat nonunion model[J]. *Bone*, 2010, 46(2): 418-424.
- [18] CHEN L, XING Q, ZHAI Q Y, et al. Pre-vascularization enhances therapeutic effects of human mesenchymal stem cell sheets in full thickness skin wound repair[J]. *Theranostics*, 2017, 7(1): 117-131.
- [19] CHEN X, CHEN Y H, HOU Y L, et al. Modulation of proliferation and differentiation of gingiva-derived mesenchymal stem cells by concentrated growth factors: potential implications in tissue engineering for dental regeneration and repair[J]. *Int J Mol Med*, 2019, 44(1): 37-46.
- [20] DOUGLAS T E L, MESSERSMITH P B, CHASAN S, et al. Enzymatic mineralization of hydrogels for bone tissue engineering by incorporation of alkaline phosphatase[J]. *Macromol Biosci*, 2012, 12(8): 1077-1089.
- [21] CHEN X, WANG J, YU L, et al. Effect of concentrated growth factor (CGF) on the promotion of osteogenesis in bone marrow stromal cells (BMSC) *in vivo*[J]. *Sci Rep*, 2018, 8(1): 5876.
- [22] 胡小敏. 浓缩生长因子在口腔颌骨再生的研究进展[J]. *临床口腔医学杂志*, 2023, 39(4): 252-255.
- [23] WINET H. The role of microvasculature in normal and perturbed bone healing as revealed by intravital microscopy[J]. *Bone*, 1996, 19(1 Suppl): 39S-57S.
- [24] 陈春燕. 细胞减少性骨髓纤维化的治疗[J]. *中国实用内科杂志*, 2023, 43(7): 540-543.
- [25] CHEN X, ZHANG R H, ZHANG Q, et al. Microtia patients: auricular chondrocyte ECM is promoted by CGF through IGF-1 activation of the IGF-1R/PI3K/AKT pathway[J]. *J Cell Physiol*, 2019, 234(12): 21817-21824.